

115. Dynamical Electroweak Symmetry

Breaking: Implications of the H^0

Updated August 2017 by K.M. Black (Boston University), R.S. Chivukula (Michigan State University), and M. Narain (Brown University).

115.1. Introduction and Phenomenology

In theories of dynamical electroweak symmetry breaking, the electroweak interactions are broken to electromagnetism by the vacuum expectation value of a composite operator, typically a fermion bilinear. In these theories, the longitudinal components of the massive weak bosons are identified with composite Nambu-Goldstone bosons arising from dynamical symmetry breaking in a strongly-coupled extension of the standard model. Viable theories of dynamical electroweak symmetry breaking must also explain (or at least accommodate) the presence of an additional composite scalar state to be identified with the H^0 scalar boson [1,2] – a state unlike any other observed so far.

Theories of dynamical electroweak symmetry breaking can be classified by the nature of the composite singlet state to be associated with the H^0 , and the corresponding dimensional scales f , the analog of the pion decay-constant in QCD, and Λ , the scale of the underlying strong dynamics.¹ Of particular importance is the ratio v/f , where $v^2 = 1/(\sqrt{2}G_F) \approx (246 \text{ GeV})^2$, since this ratio measures the expected size of the deviations of the couplings of a composite Higgs boson from those expected in the standard model. The basic possibilities, and the additional states that they predict, are described below.

115.1.1. *Technicolor*, $v/f \simeq 1$, $\Lambda \simeq 1 \text{ TeV}$:

Technicolor models [8–10] incorporate a new asymptotically free gauge theory (“technicolor”) and additional massless fermions (“technifermions” transforming under a vectorial representation of the gauge group). The global chiral symmetry of the fermions is spontaneously broken by the formation of a technifermion condensate, just as the approximate chiral symmetry in QCD is broken down to isospin by the formation of a quark condensate. The $SU(2)_W \times U(1)_Y$ interactions are embedded in the global technifermion chiral symmetries in such a way that the only unbroken gauge symmetry after chiral symmetry breaking is $U(1)_{em}$.² These theories naturally provide the Nambu-Goldstone bosons “eaten” by the W and Z boson. There would also typically be additional heavy states (e.g. vector mesons, analogous to the ρ and ω mesons in QCD) with TeV masses [14,15], and the WW and ZZ scattering amplitudes would be expected to be strong at energies of order 1 TeV.

¹ In a strongly interacting theory “Naive Dimensional Analysis” [3,4] implies that, in the absence of fine-tuning, $\Lambda \simeq g^* f$ where $g^* \simeq 4\pi$ is the typical size of a strong coupling in the low-energy theory [5,6]. This estimate is modified in the presence of multiple flavors or colors [7].

² For a review of technicolor models, see [11–13].

2 115. Dynamical electroweak symmetry breaking

There are various possibilities for the scalar H^0 in technicolor models, as described below.³ In all of these cases, however, to the extent that the H^0 has couplings consistent with those of the standard model [16], these theories are very highly constrained.

- a) **H^0 as a singlet scalar resonance:** The strongly-interacting fermions which make up the Nambu-Goldstone bosons eaten by the weak bosons would naturally be expected to also form an isoscalar neutral bound state, analogous to the σ particle expected in pion-scattering in QCD [17]. However, in this case, there is no symmetry protecting the mass of such a particle – which would therefore generically be of order the energy scale of the underlying strong dynamics Λ . In the simplest theories of this kind – those with a global $SU(2)_L \times SU(2)_R$ chiral symmetry which is spontaneously broken to $SU(2)_V$ – the natural dynamical scale Λ would be of order a TeV, resulting in a particle too heavy and broad to be identified with the H^0 . The scale of the underlying interactions could naturally be smaller than 1 TeV if the global symmetries of the theory are larger than $SU(2)_L \times SU(2)_R$, but in this case there would be additional (pseudo-)Nambu-Goldstone bosons (more on this below). A theory of this kind would only be viable, therefore, if some choice of the parameters of the high energy theory could give rise to sufficiently light state without the appearance of additional particles that should have already been observed. Furthermore, while a particle with these quantum numbers could have Higgs-like couplings to any electrically neutral spin-zero state made of quarks, leptons, or gauge-bosons, there is no symmetry insuring that the coupling strengths of such a composite singlet scalar state would be precisely the same as those of the standard model Higgs [18].
- b) **H^0 as a dilaton:** It is possible that the underlying strong dynamics is approximately scale-invariant, as inspired by theories of “walking technicolor” [19–23], and that both the scale and electroweak symmetries are spontaneously broken at the TeV energy scale [24]. In this case, due to the spontaneous breaking of approximate scale invariance, one might expect a corresponding (pseudo-) Nambu-Goldstone boson [20] with a mass less than a TeV, the dilaton.⁴ A dilaton couples to the trace of the energy momentum tensor, which leads to a similar pattern of two-body couplings as the couplings of the standard model Higgs boson [29–31]. Scale-invariance is a space-time symmetry, however, and is unrelated to the global symmetries that we can identify with the electroweak group. Therefore the decay-constants associated with the breaking of the scale and electroweak symmetries will not, in general, be the same.⁵ In other words, if there are no large anomalous dimensions associated with

³ In these models, the self-coupling of the H^0 scalar is not related to its mass, as it is in the SM – though there are currently no experimental constraints on this coupling.

⁴ Even in this case, however, a dilaton associated with electroweak symmetry breaking will likely not *generically* be as light as the H^0 [25–28].

⁵ If both the electroweak symmetry and the approximate scale symmetry are broken only by electroweak doublet condensate(s), then the decay-constants for scale and electroweak symmetry breaking may be approximately equal – differing only by terms formally proportional to the amount of explicit scale-symmetry breaking.

the W - and Z -bosons or the top- or bottom-quarks, the ratios of the couplings of the dilaton to these particles would be the same as the ratios of the same couplings for the standard model Higgs boson, but the overall strength of the dilaton couplings would be expected to be different [32,33]. Furthermore, the couplings of the dilaton to gluon- and photon-pairs can be related to the beta functions of the corresponding gauge interactions in the underlying high-energy theory, and will not in general yield couplings with the exactly the same strengths as the standard model [34,35].

- c) **H^0 as a singlet Pseudo-Nambu-Goldstone Boson:** If the global symmetries of the technicolor theory are larger than $SU(2)_L \times SU(2)_R$, there can be extra singlet (pseudo-) Nambu-Goldstone bosons which could be identified with the H^0 . In this case, however, the coupling strength of the singlet state to WW and ZZ pairs would be comparable to the couplings to gluon and photon pairs, and these would all arise from loop-level couplings in the underlying technicolor theory [36]. This pattern of couplings is not supported by the data.

115.1.2. *The Higgs doublet as a pseudo-Nambu-Goldstone Boson, $v/f < 1$, $\Lambda > 1$ TeV :*

In technicolor models, the symmetry-breaking properties of the underlying strong dynamics necessarily breaks the electroweak gauge symmetries. An alternative possibility is that the underlying strong dynamics itself does not break the electroweak interactions, and that the entire quartet of bosons in the Higgs doublet (including the state associated with the H^0) are composite (pseudo-) Nambu-Goldstone particles [37,38]. In this case, the underlying dynamics can occur at energies larger than 1 TeV and additional interactions with the top-quark mass generating sector (and possibly with additional weakly-coupled gauge bosons) cause the vacuum energy to be minimized when the composite Higgs doublet gains a vacuum expectation value [39,40]. In these theories, the couplings of the remaining singlet scalar state would naturally be equal to that of the standard model Higgs boson up to corrections of order $(v/f)^2$ and, therefore, constraints on the size of deviations of the H^0 couplings from that of the standard model Higgs [16] give rise to lower bounds on the scales f and Λ .⁶

The electroweak gauge interactions, as well as the interactions responsible for the top-quark mass, explicitly break the chiral symmetries of the composite Higgs model, and lead generically to sizable corrections to the mass-squared of the Higgs-doublet – the so-called “Little Hierarchy Problem” [41]. “Little Higgs” theories [42–45] are examples of composite Higgs models in which the (collective) symmetry-breaking structure is selected so as to suppress these contributions to the Higgs mass-squared.

⁶ In these models v/f is an adjustable parameter, and in the limit $v/f \rightarrow 1$ they reduce, essentially, to the technicolor models discussed in the previous subsection. Our discussion here is consistent with that given there, since we expect corrections to the SM Higgs couplings to be large for $v/f \simeq 1$. Current measurements constrain the couplings of the H^0 to equal those predicted for the Higgs in the standard model to about the 10% level [16], suggesting that f must have values of order a TeV or higher and, therefore, a dynamical scale Λ of at least several TeV.

4 115. Dynamical electroweak symmetry breaking

Composite Higgs models typically require a larger global symmetry of the underlying theory, and hence additional relatively light (compared to Λ) scalar particles, extra electroweak vector bosons (e.g. an additional $SU(2) \times U(1)$ gauge group), and vector-like partners of the top-quark of charge $+2/3$ and possibly also $+5/3$ [46]. In addition to these states, one would expect the underlying dynamics to yield additional scalar and vector resonances with masses of order Λ . If the theory respects a custodial symmetry [47], the couplings of these additional states to the electroweak and Higgs boson will be related – and, for example, one might expect a charged vector resonance to have similar branching ratios to WZ and WH . Different composite Higgs models utilize different mechanisms for arranging for the hierarchy of scales $v < f$ and arranging for a scalar Higgs self-coupling small enough to produce an H^0 of mass of order 125 GeV, for a review see [48]. If the additional states in these models carry color, they can provide additional contributions to Higgs production via gluon fusion [49]. The extent to which Higgs production at the LHC conforms with standard model predictions provides additional constraints (typically lower bounds on the masses of the additional colored states of order 0.7 TeV) on these models.

In addition, if the larger symmetry of the underlying composite Higgs theory does not commute with the standard model gauge group, then the additional states found in those models – especially those related to the top-quark, which tend to have the largest couplings to the electroweak sector – may be *colorless*. For example, in twin Higgs models [50], the top-partners carry no standard model charges. The phenomenology of the additional states such theories are rather different, since lacking color the production these particles at the LHC will be suppressed – and, their decays may occur only via the electroweak symmetry breaking sector, leading to their being long-lived.

115.1.3. *Top-Condensate, Top-Color, Top-Seesaw and related theories, $v/f < 1$, $\Lambda > 1$ TeV :*

A final alternative is to consider a strongly interacting theory with a high (compared to a TeV) underlying dynamical scale that *would* naturally break the electroweak interactions, but whose strength is adjusted (“fine-tuned”) to produce electroweak symmetry breaking at 1 TeV. This alternative is possible if the electroweak (quantum) phase transition is continuous (second order) in the strength of the strong dynamics [51]. If the fine tuning can be achieved, the underlying strong interactions will produce a light composite Higgs bound state with couplings equal to that of the standard model Higgs boson up to corrections of order $(1 \text{ TeV}/\Lambda)^2$. As in theories in which electroweak symmetry breaking occurs through vacuum alignment, therefore, constraints on the size of deviations of the H^0 couplings from that of the standard model Higgs give rise to lower bounds on the scale Λ . Formally, in the limit $\Lambda \rightarrow \infty$ (a limit which requires arbitrarily fine adjustment of the strength of the high-energy interactions), these theories are equivalent to a theory with a fundamental Higgs boson – and the fine adjustment of the coupling strength is a manifestation of the hierarchy problem of theories with a fundamental scalar particle.

In many of these theories the top-quark itself interacts strongly (at high energies), potentially through an extended color gauge sector [52–56]. In these theories, top-quark

condensation (or the condensation of an admixture of the top with additional vector-like quarks) is responsible for electroweak symmetry breaking, and the H^0 is identified with a bound state involving the third generation of quarks. These theories typically include an extra set of massive color-octet vector bosons (top-gluons), and an extra $U(1)$ interaction (giving rise to a top-color Z') which couple preferentially to the third generation and whose masses define the scale Λ of the underlying physics.

115.1.4. *Flavor* :

In addition to the electroweak symmetry breaking dynamics described above, which gives rise to the masses of the W and Z particles, additional interactions must be introduced to produce the masses of the standard model fermions. Two general avenues have been suggested for these new interactions. In one case, e.g. “extended technicolor” (ETC) theories [57,58], the gauge interactions in the underlying strongly interacting theory are extended to incorporate flavor. This extended gauge symmetry is broken down (possibly sequentially, at several different mass scales) to the residual strong interaction responsible for electroweak symmetry breaking. The massive gauge-bosons corresponding to the broken symmetries then mediate interactions between mass operators for the quarks/leptons and the corresponding bilinears of the strongly-interacting fermions, giving rise to the masses of the ordinary fermions after electroweak symmetry breaking. An alternative proposal, “partial compositeness” [59], the additional interactions giving rise to mixing between the ordinary quarks and leptons and massive composite fermions in the strongly-interacting underlying theory. Theories incorporating partial compositeness include additional vector-like partners of the ordinary quarks and leptons, typically with masses of order a TeV or less.

In both cases, the effects of these flavor interactions on the electroweak properties of the ordinary quarks and leptons are likely to be most pronounced in the third generation of fermions.⁷ The additional particles present, especially the additional scalars, often couple more strongly to heavier fermions.

Moreover, since the flavor interactions must give rise to quark mixing, we expect that a generic theory of this kind could give rise to large flavor-changing neutral-currents [58]. In ETC theories, these constraints are typically somewhat relaxed if the theory incorporates approximate generational flavor symmetries [60], the theory “walks” [19–23], or if $\Lambda > 1$ TeV [61]. In theories of partial compositeness, the masses of the ordinary fermions depend on the scaling-dimension of the operators corresponding to the composite fermions with which they mix. This leads to a new mechanism for generating the mass-hierarchy of the observed quarks and leptons that, potentially, ameliorates flavor-changing neutral current problems and can provide new contributions to the composite Higgs potential which allows for $v/f < 1$ [62–66].

Alternatively, one can assume that the underlying flavor dynamics respects flavor symmetries (“minimal” [67,68] or “next-to-minimal” [69] flavor violation) which suppress

⁷ Indeed, from this point of view, the vector-like partners of the top-quark in top-seesaw and little Higgs models can be viewed as incorporating partial compositeness to explain the origin of the top quark’s large mass.

flavor-changing neutral currents in the two light generations. Additional considerations apply when extending these arguments to potential explanation of neutrino masses (see, for example, [70,71]) .

Since the underlying high-energy dynamics in these theories are strongly coupled, there are no reliable calculation techniques that can be applied to analyze their properties. Instead, most phenomenological studies depend on the construction of a “low-energy” effective theory describing additional scalar, fermion, or vector boson degrees of freedom, which incorporates the relevant symmetries and, when available, dynamical principles. In some cases, motivated by the AdS/CFT correspondence [72], the strongly-interacting theories described above have been investigated by analyzing a dual compactified five-dimensional gauge theory. In these cases, the AdS/CFT “dictionary” is used to map the features of the underlying strongly coupled high-energy dynamics onto the low-energy weakly coupled dual theory [73].

More recently, progress has been made in investigating strongly-coupled models using lattice gauge theory [74]. These calculations offer the prospect of establishing which strongly coupled theories of electroweak symmetry breaking have a particle with properties consistent with those observed for the H^0 – and for establishing concrete predictions for these theories at the LHC [75].

115.2. Experimental Searches

As discussed above, the extent to which the couplings of the H^0 conform to the expectations for a standard model Higgs boson constrains the viability of each of these models. Measurements of the H^0 couplings, and their interpretation in terms of effective field theory, are summarized in the H^0 review in this volume. In what follows, we will focus on searches for the additional particles that might be expected to accompany the singlet scalar: extra scalars, fermions, and vector bosons. In some cases, detailed model-specific searches have been made for the particles described above (though generally not yet taking account of the demonstrated existence of the H^0 boson).

In most cases, however, generic searches (e.g. for extra W' or Z' particles, extra scalars in the context of multi-Higgs models, or for fourth-generation quarks) are quoted that can be used – when appropriately translated – to derive bounds on a specific model of interest.

The mass scale of the new particles implied by the interpretations of the low mass of H^0 discussed above, and existing studies from the Tevatron and lower-energy colliders, suggests that only the Large Hadron Collider has any real sensitivity. A number of analyses already carried out by ATLAS and CMS use relevant final states and might have been expected to observe a deviation from standard model expectations – in no case so far has any such deviation been reported. The detailed implications of these searches in various model frameworks are described below.

Except where otherwise noted, all limits in this section are quoted at a confidence level of 95%. The searches at $\sqrt{s} = 8$ TeV (Run 1) are based on 20.3 fb^{-1} of data recorded by ATLAS, and an integrated luminosity of 19.7 fb^{-1} analyzed by CMS. The datasets

collected at $\sqrt{s} = 13$ TeV during Run 2 of the LHC since 2015 are based on analyses with varied integrated luminosities ranging between $\sim 2\text{--}36\text{fb}^{-1}$.

115.2.1. Searches for Z' or W' Bosons :

Massive vector bosons or particles with similar decay channels would be expected to arise in Little Higgs theories, in theories of Technicolor, or models involving a dilaton, adjusted to produce a light Higgs boson, consistent with the observed H^0 . These particles would be expected to decay to pairs of vector bosons, to third generation quarks, or to leptons. The generic searches for W' and Z' vector bosons listed below can, therefore, be used to constrain models incorporating a composite Higgs-like boson.

A general review of searches for Z' and W' bosons is also included in this volume [76,77]. In the context of the dynamical electroweak symmetry breaking models, we emphasize their decays to third generation fermions by including a detailed overview, while also briefly summarizing the other searches.

$Z' \rightarrow \ell\ell$:

ATLAS [78] and CMS [79] have both searched for Z' production with $Z' \rightarrow ee$ or $\mu\mu$. No deviation from the standard model prediction was seen in the dielectron and dimuon invariant mass spectra, by either the ATLAS or the CMS analysis, and lower limits on possible Z' boson masses were set. A Z'_{SSM} with couplings equal to the standard model Z (a “sequential standard model” Z') and a mass below 4.5 TeV was excluded by ATLAS, while CMS set a lower mass limit of 4.0 TeV. The experiments also place limits on the parameters of extra dimension models and in the case of ATLAS on the parameters of a minimal walking technicolor model [19–23], consistent with a 125 GeV Higgs boson [80]. For a general review of searches in these channels see the PDG review of Z prime in this volume [76].

In addition, both experiments have also searched for Z' decaying to a ditau final state [81,82]. While less sensitive than dielectron or dimuon final states, an excess in $\tau^+\tau^-$ could have interesting implications for models in which lepton universality is not a requirement and enhanced couplings to the third generation are allowed. This analysis led to lower limits on the mass of a Z'_{SSM} of 2.4 and 2.1 TeV from ATLAS and CMS respectively.

$Z' \rightarrow q\bar{q}$:

The ability to relatively cleanly select $t\bar{t}$ pairs at the LHC together with the existence of enhanced couplings to the third generation in many models makes it worthwhile to search for new particles decaying in this channel. Both ATLAS [84] and CMS [83] have carried out searches for new particles decaying into $t\bar{t}$.

ATLAS focused on the lepton plus jets final state, where the top quark pair decays as $t\bar{t} \rightarrow WbWb$ with one W boson decaying leptonically and the other hadronically; CMS used final states where both, one or neither W decays leptonically and then combined the results. The $t\bar{t}$ invariant mass spectrum was analyzed for any excess, and no evidence for any resonance was seen. ATLAS excluded a narrow ($\Gamma/m = 1.2\%$) leptophobic top-color Z' boson with masses between 0.7 and 2.1 TeV and with $\Gamma/m = 3\%$ between 0.7 and 3.2 TeV. CMS set limits on leptophobic Z' bosons for three different assumed widths

8 115. Dynamical electroweak symmetry breaking

$\Gamma/m = 1.0\%$, $\Gamma/m = 10.0\%$, and $\Gamma/m = 30.0\%$ of 3.9 TeV to 4.0 TeV and exclude RS KK gluons up to 3.3 TeV.

Both ATLAS [85] and CMS [86] have also searched for resonances decaying into $q\bar{q}$, qg or gg using the dijet invariant mass spectrum. Model-independent upper limits on cross sections were set; ATLAS excluded Z' bosons below 2.1 TeV, W' bosons below 3.6 TeV and chiral W^* bosons below 3.4 TeV. CMS was able to exclude W' bosons below 2.7 TeV; Z' bosons below 2.1 TeV and between 2.3 and 2.6 TeV; color octet scalars below 3.0 TeV; and g_{KK} gravitons below 1.9 TeV. Searches were also carried out for wide resonances, assuming Γ/m up to 30%, and excluded axigluons and colorons with mass below 5.5 TeV. Additionally ATLAS [87] and CMS [88] searched for $Z' \rightarrow b\bar{b}$ selecting events where at least one of the jets is b-tagged. ATLAS excluded Z' bosons in the range of 1.1 to 1.5 TeV while CMS excluded masses between 1.2 and 1.68 TeV.

$W' \rightarrow \ell\nu$:

Both LHC experiments have also searched for massive charged vector bosons. In this section we include a summary of the results, with emphasis on final states with third generation fermions, while the details on other decays are discussed in the mini-review of W' [77]. ATLAS searched for a heavy W' decaying to $e\nu$ or $\mu\nu$ and find no excess over the standard model expectation. A sequential standard model (SSM) W' boson (assuming zero branching ratio to WZ) with mass less than 5.1 TeV was excluded [89] using 36 fb^{-1} dataset at $\sqrt{s} = 13 \text{ TeV}$, and excited chiral bosons W^* excluded up to 3.21 TeV [90] (20.3 fb^{-1} , $\sqrt{s} = 8 \text{ TeV}$). Based on a smaller dataset, the CMS experiment excluded a SSM W' boson with mass up to 4.1 TeV [91] and presented the upper limits on the production of generic W' bosons decaying into this final state using a model-independent approach.

CMS [92] has carried out a complementary search in the $\tau\nu$ final state. As noted above, such searches place interesting limits on models with enhanced couplings to the third generation. No excess was observed and limits between 2.0 and 2.7 TeV were set on the mass of a W' decaying preferentially to the third generation; a W' with universal fermion couplings was also excluded for masses less than 2.7 TeV.

$W' \rightarrow t\bar{b}$:

Heavy new gauge bosons can couple to left-handed fermions like the SM W boson or to right-handed fermions. W' bosons that couple only to right-handed fermions (W'_R) may not have leptonic decay modes, depending on the mass of the right-handed neutrino. For these W' bosons, the $t\bar{b}$ ($t\bar{b} + \bar{t}b$) decay mode is especially important because in many models the W' boson is expected to have enhanced couplings to the third generation of quarks relative to those in the first and second generations. It is also the hadronic decay mode with the best signal-to-background. ATLAS and CMS have performed searches for W' bosons via the $W' \rightarrow t\bar{b}$ decay channel in the lepton+jets and all-hadronic final state.

The CMS lepton+jets search [93,94,95,96], $W' \rightarrow t\bar{b} \rightarrow Wbb \rightarrow \ell\nu bb$, proceeded via selecting events with an isolated lepton (electron or muon), and at least two jets, one of which is identified to originate from a b-quark. The mass of the W' boson ($M_{t\bar{b}}$) was reconstructed using the four-momentum vectors of the final state objects ($b\bar{b}\ell\nu$). The distribution of $M_{t\bar{b}}$ is used as the search discriminant. A search [96] using 35.9 fb^{-1} of

data, collected at $\sqrt{s} = 13$ TeV, led to an exclusion of W'_R bosons with masses below 3.4 TeV (3.6 TeV) if $M_{W'_R} \gg M_{\nu_R}$ ($M_{W'_R} < M_{\nu_R}$), where M_{ν_R} is the mass of the right-handed neutrino.

The CMS search for $W' \rightarrow t\bar{b}$ decays using the all-hadronic final state focused on W' masses above 1 TeV [95]. In this region, the top quark gets a large Lorentz boost and hence the three hadronic products from its decay merge into a single large-radius jet. Techniques which rely on substructure information of the jets [97] are employed to identify boosted W and top quark jets and compute the mass of the jet. W' candidate mass was computed from back-to-back boosted top tagged jet and a low mass b tagged jet. From this all-hadronic search, W' bosons were excluded for masses up to 2.02 TeV.

ATLAS has searched for W'_R bosons in the $t\bar{b}$ final state both for lepton+jets [98] and all-hadronic [99] decays of the top. No significant deviations from the standard model were seen in either analysis and limits were set on the $W' \rightarrow t\bar{b}$ cross section times branching ratio and W' bosons with purely left-handed (right-handed) couplings to fermions were excluded for masses below 1.70 (1.92) TeV.

In addition, the above studies also provided upper limits on the W' effective couplings to right- and left-handed fermions. In Fig. 115.1 (bottom) the upper limits on W' couplings normalized to the SM W couplings derived by ATLAS [98] are shown. The top panel of Fig. 115.1 shows the upper limits for arbitrary combinations of left- and right-handed couplings of the W' boson to fermions set using a model independent approach by CMS [96].

115.2.2. *Searches for Resonances decaying to Vector Bosons and/or Higgs Bosons :*

$X \rightarrow WW, WZ, ZZ:$

Both the ATLAS and CMS experiments have used the data collected at $\sqrt{s} = 8$ TeV and $\sqrt{s} = 13$ TeV to search for resonances decaying to pairs of bosons. Overall no significant excesses were seen in the full datasets that were analyzed and the results are interpreted in models with heavy vector triplets (HVT) [100], models with strong gravity and extra spatial dimensions, as well as setting model independent limits as a function of mass. For a full review of models including extra spatial dimensions including the interpretation of many of these results in that context please see the review of extra dimensions in this volume [73].

Utilizing data collected at $\sqrt{s} = 8$ TeV, ATLAS [101] and CMS [102] have both looked for a resonant state (such as a W') decaying to WZ in the fully-leptonic channel, $\ell\nu\ell'\ell'$ (where $\ell, \ell' = e, \mu$). The WZ invariant mass distribution reconstructed from the observed lepton momenta missing transverse energy. The backgrounds arise mainly from standard model WZ , ZZ and $t\bar{t} + W/Z$ production. No significant deviation from the standard model prediction is observed by either experiment. A W' with mass less than 1.55 (1.52) TeV is excluded by CMS (ATLAS); ATLAS also sets limits on the production cross section for HVT particles, and CMS sets limits on the production of low-scale technimesons ρ_{TC} from the reconstructed WZ mass spectrum and cross section.

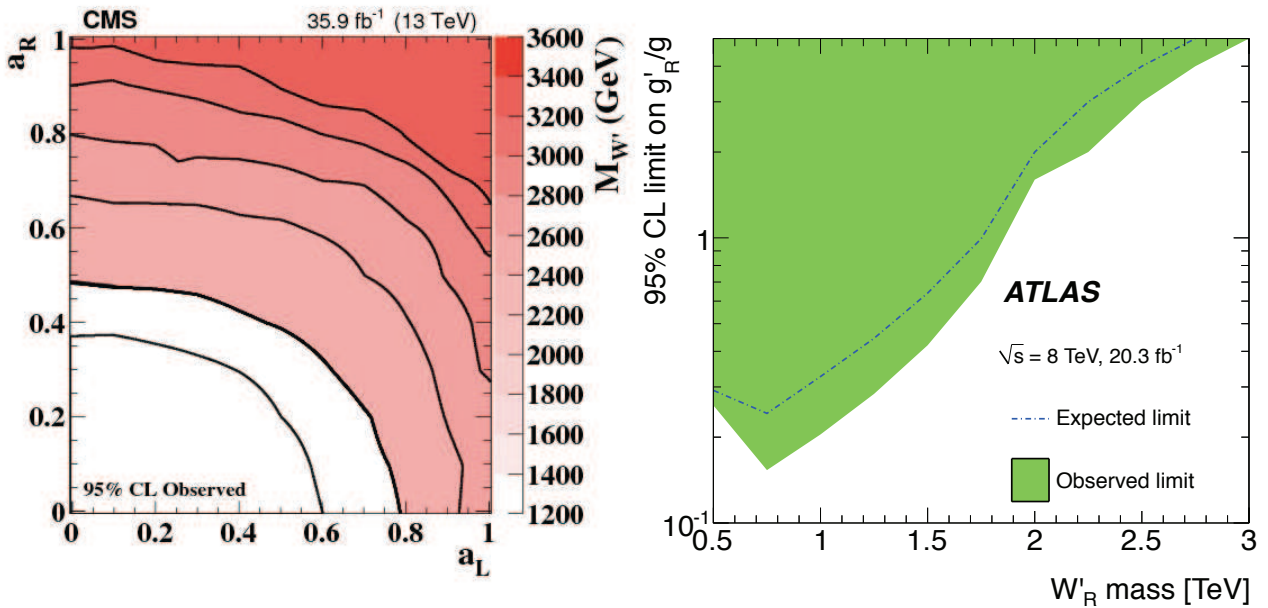


Figure 115.1: Left panel: Observed limits on the W' boson mass as function of the left-handed (a_L) and right-handed (a_R) couplings. Black lines represent contours of equal W' boson mass [96]. Right panel: Observed and expected regions, on the g'/g vs mass of the W' -boson plane, that are excluded at 95% CL, for right-handed W' bosons [98].

ATLAS [103,104] and CMS [105] have also searched for narrow resonances decaying to WW , WZ or ZZ in $lvjj$ and $\ell\ell jj$ final states (where one boson decays leptonically and the other to jets) in data recorded at $\sqrt{s} = 13$ TeV. No deviation from the standard model is seen by either experiment; resonance masses below 2.750 TeV for a HVT model decaying into WW and 2.820 TeV decaying into WZ by ATLAS and below 2.4 TeV by CMS.

Searches have also been conducted in fully hadronic final states. ATLAS [106] and CMS [107] have searched for massive resonance in dijet systems with one or both jets identified as a W or a Z boson using jet-substructure techniques. Limits are set by both experiments on the production cross section times branching ratio for new HVT particles decaying to WZ and ZZ and for g_{KK} gravitons decaying to WW or ZZ . ATLAS excludes HVT particles between 1.2 and 3.5 TeV while CMS excludes W' bosons below 3.6 TeV and Z' bosons below 2.7 TeV.

$X \rightarrow W/Z + H^0$ and $X \rightarrow H^0 H^0$:

With the existence and decay properties of the Higgs boson established, and the significant datasets now available, it is possible to use searches for anomalous production of the Higgs as a potential signature for new physics. ATLAS [108,109] and CMS [110,111] have both searched in the data collected at $\sqrt{s} = 13$ TeV for new particles decaying

to a vector boson plus a Higgs boson, where the vector boson decays leptonically or hadronically and the Higgs boson to $b\bar{b}$. No deviation from the standard model is seen in any of these final states and limits can be placed on the allowed production cross section times branching ratio for resonances on a heavy vector triplet model. The exact limits depend on the parameters considered but exclude HVT particles with a mass up to 3.8 TeV. Both experiments also place model-independent limits on the production cross-section as a function of mass.

Both experiments [112,113,114] have also searched for resonant production of Higgs boson pairs $X \rightarrow H^0 H^0$ with $H^0 \rightarrow b\bar{b}$. No signal is observed and limits are placed on the possible production cross section for any new resonance and cross-section limits are placed between 1000 fb and 2 fb for masses between 0.3 and 3.0 TeV on resonant production. ATLAS additionally places limits on non-resonant Standard Model Higgs production constrained to be less than 330 fb.

$Y \rightarrow W/Z + X$ with $X \rightarrow jj$:

ATLAS has searched for a dijet resonance [115] with an invariant mass in the range 130 – 300 GeV, produced in association with a W or a Z boson. The analysis used 20.3 fb⁻¹ of data recorded at $\sqrt{s} = 8$ TeV. The W or Z boson is required to decay leptonically ($\ell = e, \mu$). No significant deviation from the standard model prediction is observed and limits are set on the production cross section times branching ratio for a hypothetical technipion produced in association with a W or Z boson from the decay of a technirho particle in the context of Low Scale Technicolor models.

ATLAS [116] has searched for a resonance (Y) decaying into XH where $H \rightarrow b\bar{b}$ and a new particle X decays into dijet pairs ($X \rightarrow jj$). A two dimensional scan in both Y , between 1 and 4 TeV, and X masses, between 0.05 and 1 TeV is performed. No significant excesses are seen and upper limits on the cross-section of this process are set as a function of X and Y .

Summary of Searches with Diboson Final States:

Both ATLAS [117] and CMS [118] provide plots summarizing the various searches results and limits. The results are shown in the context of HVT models and models of strong gravity with extra spatial dimensions. No excess is seen in any search and limits on the W' are placed up to 3.5 TeV and 2.7 TeV on Z' particles in the HVT model as seen in Fig. 115.2

115.2.3. Vector-like third generation quarks :

Vector-like quarks (VLQ) have non-chiral couplings to W bosons, i.e. their left- and right-handed components couple in the same way. They therefore have vectorial couplings to W bosons. Vector-like quarks arise in Little Higgs theories, top-coloron-models, and theories of a composite Higgs boson with partial compositeness. In the following, the notation T quark refers to a vector-like quark with charge 2/3 and the notation B quark refers to a vector-like quark with charge $-1/3$, the same charges as the SM top and b quarks respectively. The X and Y have charges 5/3, and $-4/3$ respectively. Vector-like quarks couple with SM quarks with Yukawa interactions and may exist as $SU(2)$ singlets (T , and B), doublets $[(X, T), (T, B), (B, Y)]$, or triplets $[(X, T, B), (T, B, Y)]$. At the

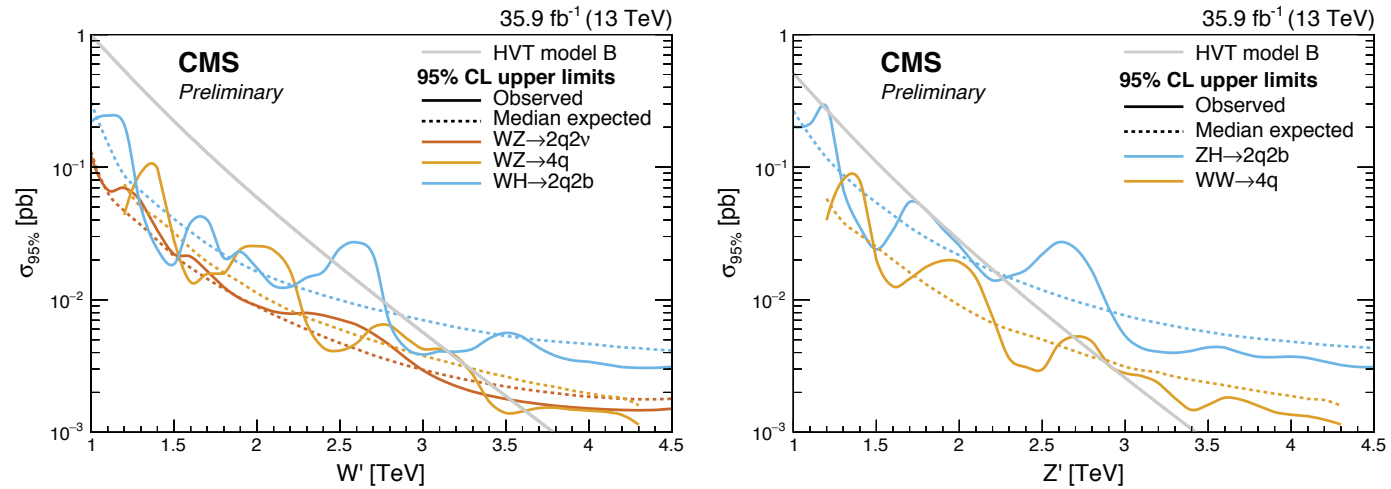


Figure 115.2: Left panel: Observed limits from W' to diboson from CMS [118]. Right panel: Observed limits from Z' to diboson decays from CMS [118]. Note in both cases ATLAS provides similar summary plots which are available [117].

LHC, VLQs can be pair produced via the dominant gluon-gluon fusion. VLQs can also be produced singly by their electroweak effective couplings to a weak boson and a standard model quark. Single production rate is expected to dominate over the rate of pair production at large VLQ masses. T quarks can decay to bW , tZ , or tH^0 . Weak isospin singlets are expected to decay to all three final states with (asymptotic) branching fractions of 50%, 25%, 25%, respectively. Weak isospin doublets are expected to decay exclusively to tZ and to tH^0 [119] with equal branching ratios. Analogously, B quarks can decay to tW , bZ , or bH^0 . The Y and X quarks decay exclusively to bW and to tW . While these are taken as the benchmark scenarios, other representations are possible and hence the final results are interpreted for many allowed branching fraction combinations.

Given the multiple decay modes of the VLQs, the final state signatures of both pair produced and the singly produced VLQs are fairly rich with leptons, jets, b-jets, and missing energy. Depending on the mass of the VLQ, the top quarks and $W/Z/H^0$ bosons may be Lorentz boosted and identified using jet substructure techniques. Thus the searches are performed using lepton+jets signatures, multi-lepton and all-hadronic decays. In addition, T or B quarks with their antiparticles can result in events with same-sign leptons, for example if the decay $T \rightarrow tH \rightarrow bWW^+W^-$ is present, followed by leptonic decays of two same-sign W bosons. In the following subsections, while we describe the searches for each of the decay modes of the VLQs, the same analysis can be re-interpreted to obtain the sensitivity to a combination with varied branching fractions to the different decay modes.

In the following sections, the results obtained for T (B) quarks assuming 100% branching ratio to Wb (Wt) are also applicable to heavy vector-like Y (X) with charge $4/3$ ($5/3$).

115.2.3.1. *Searches for T quarks that decay to W , Z and H^0 bosons:* $T/Y \rightarrow bW$:

CMS has searched for pair production of heavy T quarks that decay exclusively to bW [120,121,122]. The analysis selected events with exactly one charged lepton, assuming that the W boson from the second T quark decays hadronically. Under this hypothesis, a 2-constraint kinematic fit can be performed to reconstruct the mass of the T quark. In Ref. 121 and Ref. 122, the two-dimensional distribution of reconstructed mass vs S_T was used to test for the signal. S_T is the scalar sum of the missing p_T and the transverse momenta of the lepton and the leading four jets. This analysis, when combined with the search in the fully hadronic final state [123] excluded new quarks that decay 100% to bW for masses below 0.89 TeV [122]. At times the hadronically-decaying W boson is produced with a large Lorentz boost, leading to the W decay products merged into a wide single jet also known as a fat jet. Algorithms such as jet pruning [124] were used to resolve the substructure of the fat jets from the decays of the heavy particles. If the mass of the boosted jet was compatible with the W boson mass, then the W boson candidate jet and its subjets were used in the kinematic reconstruction of the T quark. No excess over standard model backgrounds was observed. Upper limits on the production cross section as a function of the mass of T quarks were measured. By comparing them with the predicted cross section for vector like quark pair production, the strong pair production of T quarks was excluded for masses below 1.30 TeV (1.28 TeV expected) [120].

An analogous search has been carried out by ATLAS [125], [126] for the pair production of heavy T quarks. It used the lepton+jets final state with an isolated electron or muon and at least four jets, including a b-jet and required reconstruction of the T quark mass. Given the mass range of the T quark being explored was from a 0.4 TeV to a couple of TeV, the W boson from the T quark may fall in two categories: those with a high boost leading to merged decay products, and others where the two jets from the W boson were resolved. In addition, the selection was optimized to require large angular separation between the high p_T W bosons and the b-jets. The $T \rightarrow Wb$ candidates were constructed from both the leptonically and hadronically decaying W bosons by pairing them with the two highest p_T b-tagged jets in the event. The pairing of b-jets with W bosons which minimizes the difference between the masses of leptonically decaying T ($m_{lep}(T)$) and the hadronic T ($m_{had}(T)$) was chosen. Finally, $m_{lep}(T)$ was used as the discriminating variable in a signal region defined by high S_T , the scalar sum of the missing p_T , the p_T of the lepton and jets, and the opening angle between the lepton and the neutrino ($\Delta R(e, \nu)$). With the 36.1fb^{-1} data collected during Run 2 at $\sqrt{s} = 13$ TeV, assuming 100% branching ratio to the Wb decay, the observed lower limit on the T mass was 1.35 TeV, and in the SU(2) singlet scenario, the lower mass limit was obtained to be 1.17 TeV [125].

A targeted search for a T quark, produced singly in association with a light flavor quark and a b quark and decaying into bW , was carried out by CMS at $\sqrt{s}=13$ teV and a dataset corresponding to 2.3fb^{-1} [127]. The analysis used lepton+jets events, with at least one b-tagged jet with large transverse momentum, and a jet in the forward η region. Selected events were required to have $S_T > 500$ GeV, where S_T is defined

as the scalar sum of the transverse momenta of the lepton, the leading central jet, and the missing transverse momentum. The invariant mass of the T candidate was used as the discriminating variable and was reconstructed using the four-vectors of the leptonically decaying W boson and the leading central jet. No excess over the standard model prediction was observed. As the VLQ width is proportional to the square of the coupling, upper limits were set on the production cross section assuming a narrow width VLQ with coupling greater than 0.5. For Y/T quarks with a coupling of 0.5 and a 100% branching fraction for the decay to bW the excluded masses were in the range from 0.85 to 1.40 TeV [127]. A similar search [128,129] performed by ATLAS, for singlet T quarks, with coupling of $\sqrt{(c_L^{Wb})^2 + (c_R^{Wb})^2} = \frac{1}{\sqrt{2}}$, and $\mathcal{B}(T \rightarrow bW) = 0.5$, led to exclusion limits on T/Y masses below 1.44 TeV. This search also provided limits, as a function of the Y quark mass, on the coupling of the Y quark to bW , and the mixing parameter $|\sin\theta_R|$ for a (Y,B) doublet model [128]. For a VLQ mass around 1 TeV, the smallest excluded coupling-strength values are obtained, with $|c_L^{Wb}|=0.45$ for a T quark and $\sqrt{(c_L^{Wb})^2 + (c_R^{Wb})^2}=0.33$ for a Y quark. The limit on $|\sin\theta_R|$ is around 0.23, and close to the constraints from electroweak precision observables.

$T \rightarrow tH^0$:

ATLAS has performed a search for $T\bar{T}$ production with $T \rightarrow tH^0$ [126], [130]. Given the dominant decay mode $H^0 \rightarrow b\bar{b}$, these events are characterized by a large number of jets, many of which are b-jets. Thus the event selection required one isolated electron or muon and high jet multiplicity (including b tagged jets). The sample is categorized by the jet multiplicity (5 and ≥ 6 jets in the 1-lepton channel; 6 and ≥ 7 jets in the 0-lepton channel), b-tag multiplicity (2, 3 and ≥ 4) and mass-tagged jet multiplicity (0, 1 and ≥ 2). The distribution of m_{eff} , defined as the scalar sum of the lepton and jet p_T s and the missing E_T , for each category were used as the discriminant for the final signal and background separation. No excess of events were found. Weak isospin doublet T quarks were excluded below 1.16 TeV.

The CMS search for $T\bar{T}$ production, with $T \rightarrow tH^0$ decays has been performed in both lepton+jets, multilepton and all hadronic final states. The lepton+jets analysis [131] emphasizes the presence of large number of b-tagged jets, and combined with other kinematic variables in a Boosted Decision Tree (BDT) for enhancing signal to background discrimination. The multilepton analysis [131] was optimized for the presence of b-jets and the large hadronic activity. For $\mathcal{B}(T \rightarrow Wb) = 1$, the combined lepton+jets and multilepton analyses led to a lower limit on T quark masses of 0.71 TeV. A search for $T \rightarrow tH^0$ in all hadronic decays [132], optimized for a high mass T quark, and based on identifying boosted top quark jets has been carried out by CMS. This search aimed to resolve sub-jets within the jets arising from boosted top quark decays, including b-tagging of the sub-jets. A likelihood discriminator was defined based on the distributions of H_T , and the invariant mass of the two b-jets in the events for signal and background. No excess above background expectations was observed. Assuming 100% branching ratio for $T \rightarrow tH^0$, this analysis led to a lower limit of 0.75 TeV on the mass of the T quark.

Searches for T quarks at $\sqrt{s}=13$ TeV, based on a 2.6fb^{-1} dataset [133] have been performed by CMS using the lepton+jets final state. This search has been optimized for

high mass T quarks by exploiting techniques to identify W or Higgs bosons decaying hadronically with large transverse momenta. The boosted W channel excluded T quarks decaying only to bW with masses below 0.91 TeV, and the boosted tH channel excluded T quarks decaying only to tH for masses below 0.89 TeV.

A CMS search for $T \rightarrow tH^0$ with $H^0 \rightarrow \gamma\gamma$ decays has been performed [134] in pair production of T quarks. To identify the Higgs boson produced in the decay of the heavy T quark, and the subsequent $H^0 \rightarrow \gamma\gamma$ decay, the analysis focused on identification of two photons in events with one or more high p_T lepton+jets or events with no leptons and large hadronic activity. A search for a resonance in the invariant mass distribution of the two photons in events with large hadronic activity defined by the H_T variable showed no excess above the prediction from standard model processes. The analysis resulted in exclusion of T quark masses below 0.54 TeV.

A search for electroweak single production of T quark decaying to tH^0 using boosted topologies in fully hadronic [135] and lepton+jets [136] in the final states has been performed by CMS. The electroweak couplings of the T quarks to the SM third generation quarks are highly model dependent and hence these couplings determine the rates of the single T quark production. In both analyses, T quark candidate invariant mass was reconstructed using the boosted Higgs boson jets and the top quark. Higgs boson jets were identified using jet substructure techniques and subjet b tagging. For the lepton+jets analysis the top quark was reconstructed from the leptonically decaying W and the b jet, while in the all hadronic analysis the top quark jet was tagged using substructure analysis. There was no excess of events observed above background. Exclusion limits on the product of the production cross section and the branching fraction ($\sigma(pp \rightarrow Tqt/b) \times \mathcal{B}(T \rightarrow tH^0)$) were derived for the T quark masses in the range 0.70-1.8 TeV. From the lepton+jets analysis, for a mass of 1.0 TeV, values of ($\sigma(pp \rightarrow Tqt/b) \times \mathcal{B}(T \rightarrow tH^0)$) greater than 0.8 and 0.7 pb were excluded assuming left- and right-handed coupling of the T quark to standard model fermions, respectively [136]. For the all-hadronic analysis, upper limits between 0.31 and 0.93 pb were obtained on ($\sigma(pp \rightarrow Tqt/b) \times \mathcal{B}(T \rightarrow tH^0)$) for T quark masses in the range 1.0-1.8 TeV [135].

$T \rightarrow tZ$:

Both ATLAS and CMS search for T quarks that decay exclusively into tZ in pp collisions at $\sqrt{s} = 13$ TeV. No excesses were found in either search.

ATLAS performed a search [137] for optimized pair production of vector-like top quarks decaying into tZ where the Z boson subsequently decays into neutrino pairs utilizing 36.1 fb^{-1} of data. The search selected events with one lepton, multiple jets, and significant missing transverse momentum. No significant excesses were found and lower limits on the mass of a vector like top quark were placed, excluding masses below 0.87 TeV (weak-isospin singlet), 1.05 TeV (weak-isospin doublet), and 1.16 TeV (pure Zt mode). CMS searched [138] for single production of T quarks decaying into tZ with the Z boson decaying to pairs of charged leptons (electrons and muons) and the top quark decaying hadronically using 35.9 fb^{-1} of data. Limits were placed on T quarks with masses between 0.7 and 1.7 TeV excluding the product of cross-section and branching

fraction above values of 0.27 to 0.04 pb. Additionally, limits on a Z' boson decaying into tZ were set.

Combined searches for $T \rightarrow bW/tZ/tH^0$:

Most of the analyses described above targeted an individual decay mode of the T quark, with 100% branching ratio to either bW , tZ or tH^0 and were optimized accordingly. However, they have varied sensitivity to all three decay modes and the results can be interpreted as a function of branching ratios to each of the three decay modes, with the total adding up to unity ($\mathcal{B}(tH) + \mathcal{B}(tZ) + \mathcal{B}(Wb) = 1$).

Combinations of analyses are performed by both ATLAS and CMS. The limits set by ATLAS searches in lepton+jets, dileptons with same-sign charge, and final states with Z boson have been combined and the results obtained for various sets of branching fractions for T quark decays to bW , tH^0 and tZ are shown in Fig. 115.3. In the combined analysis, ATLAS set lower T quarks mass limits that ranged from 0.6 to 1.35 TeV for all possible values of the branching fractions to the three decay modes [125,139]. In Fig. 115.3, exclusion is shown in the plane of $\mathcal{B}(T \rightarrow Ht)$ versus $\mathcal{B}(T \rightarrow Wb)$, for different values of the T quark mass from the lepton+jets analyses optimized for bW , tH , Zt modes and the same-sign leptons analysis. The grey (light shaded) area in the figure corresponds to the unphysical region where the sum of branching ratios exceeds unity, or is smaller than zero. The default branching ratio values for the weak-isospin singlet and doublet cases are also shown in Fig. 115.3 as cross and square symbols respectively. A similar combination was also performed by CMS.

An inclusive search by CMS targeted at heavy T quarks decaying to any combination of bW , tZ , or tH^0 is described in Ref. 131. Selected events have at least one isolated charged lepton. Events were categorized according to number and flavour of the leptons, the number of jets, and the presence of hadronic vector boson and top quark decays that are merged into a single jet. The use of jet substructure to identify hadronic decays significantly increases the acceptance for high T quark masses. No excess above standard model backgrounds was observed. Limits on the pair production cross section of the new quarks are set, combining all event categories, for all combinations of branching fractions into the three final states. For T quarks that exclusively decay to $bW/tZ/tH^0$, masses below 0.70/0.78/0.71 TeV are excluded.

115.2.3.2. *Searches for B quarks that decay to W , Z and H^0 bosons:*

ATLAS and CMS have performed searches for pair production of heavy B quarks which subsequently decay to Wt , bZ or bH^0 . The searches have been carried out in final states with single leptons, di-leptons (with same charge or opposite charge), multileptons, as well as in fully hadronic final states.

$B \rightarrow WtX$:

A search for $B \rightarrow tW$ has been performed by the ATLAS experiment [125] using lepton+jets events with one hadronically decaying W and one leptonically decaying W utilizing 36.1 fb^{-1} of data at $\sqrt{s} = 13 \text{ TeV}$. The search was optimized for T production decaying into Wb . Since the analysis was optimized for $T \rightarrow Wb$ rather than Wt decays the analysis does not reconstruct the full B mass. As discussed earlier, the hadronically

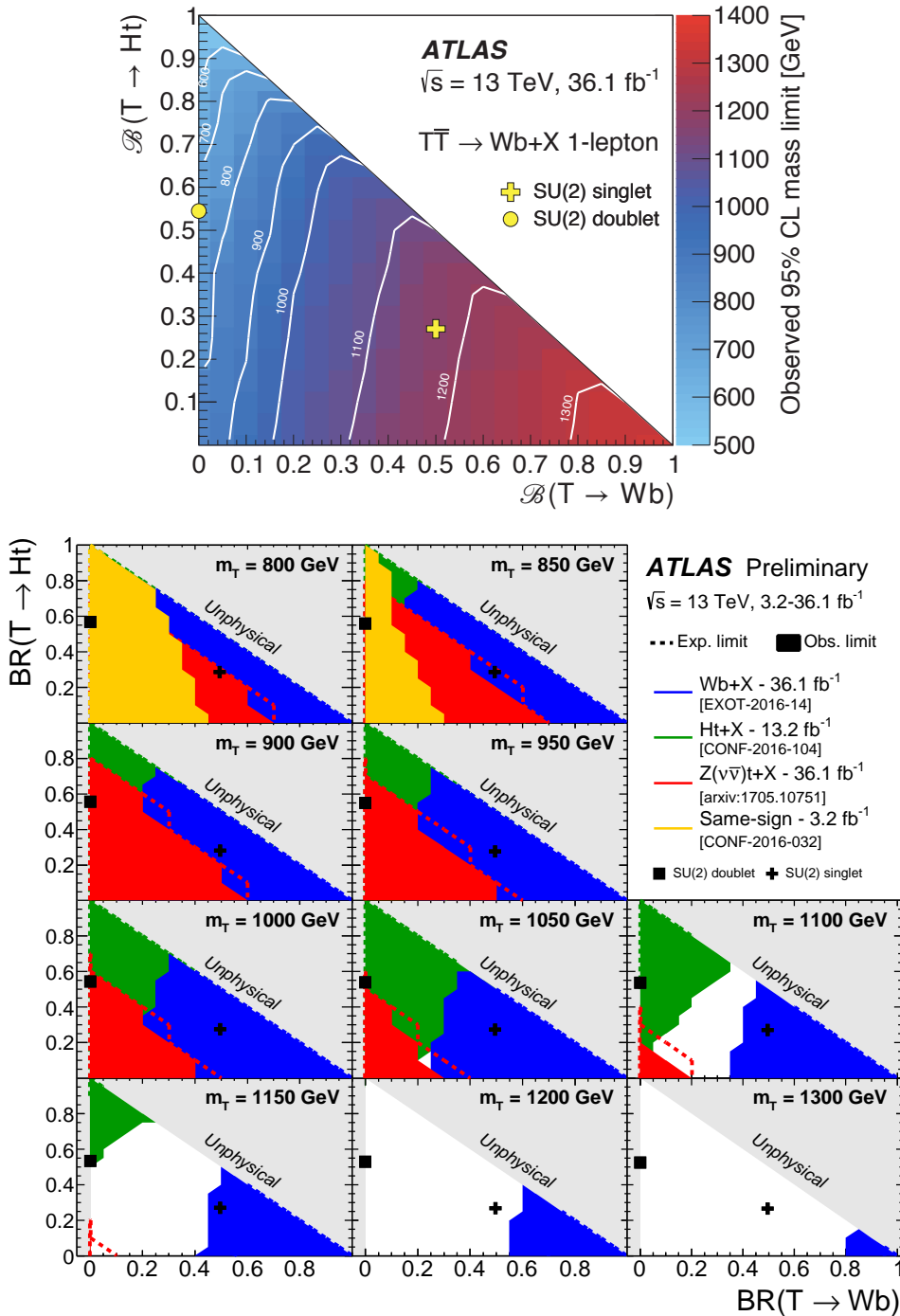


Figure 115.3: Observed limits on the mass of the T quark in the plane of $\mathcal{B}(T \rightarrow tH^0)$ versus $\mathcal{B}(T \rightarrow bW)$ from all ATLAS searches for TT production. The markers indicate the default branching ratios for the SU(2) singlet and doublet scenarios with masses above 0.8 TeV, where they are approximately independent of the VLQ T mass. Top panel: Summary from the $T \rightarrow Wb$ analysis [125]. Bottom panel: Exclusions for different T quark masses for the $Wb+X$ (blue), the tH^0+X (green), the $Z(\nu\bar{\nu})t+X$ (red) and the same-sign leptons (yellow) analyses. Similar combination plots are also made by CMS.

and leptonically decaying heavy quarks were required to have similar reconstructed masses (within 300 GeV). The interpretation of the $T \rightarrow Wb$ in the context of $B \rightarrow tW$ production led to the exclusion of Heavy B like VLQs for masses less than 1.25 TeV and 1.08 TeV, assuming a 100% branching fraction to tW or SU(2) singlet B scenario, respectively.

A similar search by CMS [140], using 19.8 fb^{-1} of $\sqrt{s} = 8 \text{ TeV}$ data, selected events with one lepton and four or more jets, with at least one b-tagged jet, significant missing p_T , and further categorizes them based on the number of jets tagged as arising from the decay of boosted W , Z or H^0 bosons. The S_T distributions of the events in different categories showed no excess of events above the expected background and yielded a lower limit on the B quark mass of 0.73 TeV for $BR(B \rightarrow Wt) = 1$.

CMS [133] also searches for pair production of both TT and BB with collisions from 2.5 fb^{-1} of $\sqrt{s} = 13 \text{ TeV}$ data. The analysis searches for events with one high p_T lepton, multiple jets, and highly boosted W or Higgs bosons decaying hadronically. The analysis focuses on pair production and selects events with either a boosted W or Higgs candidate and then proceeds to search for anomalous production in excess of standard model production. Seeing no significant excesses CMS then proceeded to set limits in many different interpretations. The strongest was from the the $B \rightarrow Wt$ interpretation leading to excluding heavy vector like B's less than 0.73 TeV.

$B \rightarrow bZX$:

A search by CMS [141] for the pair-production of a heavy B quark and its antiparticle, one of which decays to bZ , selected events with a Z -boson decay to e^+e^- or $\mu^+\mu^-$ and a jet identified as originating from a b quark. The signal from $B \rightarrow bZ$ decays would appear as a local enhancement in the bZ mass distribution. No such enhancement was found and B quarks that decay 100% into bZ are excluded below 0.70 TeV. This analysis also set upper limits on the branching fraction for $B \rightarrow bZ$ decays of 30-100% in the B quark mass range 0.45-0.70 TeV. A complementary search has been carried out by ATLAS for new heavy quarks decaying into a Z boson and a b-quark [142]. Selected dilepton events contain a high transverse momentum Z boson that decays leptonically, together with two b-jets. If the dilepton events have an extra lepton in addition to those from the Z boson, then only one b-jet is required. No significant excess of events above the standard model expectation was observed, and mass limits were set depending on the assumed branching ratios, see Fig. 115.4. In a weak-isospin singlet scenario, a B quark with mass lower than 0.65 TeV was excluded, while for a particular weak-isospin doublet scenario, a B quark with mass lower than 0.73 TeV was ruled out.

ATLAS has searched for the electroweak production of single B quarks, which is accompanied by a b-jet and a light jet [142]. The dilepton selection for double B production was modified for the single B production study by requiring the presence of an additional energetic jet in the forward region. An upper limit of 200 fb was obtained for the process $\sigma(pp \rightarrow B\bar{b}q) \times B(B \rightarrow Zb)$ with a heavy B quark mass at 0.70 TeV. This search indicated that the electroweak mixing parameter X_{Bb} below 0.5 is neither expected or observed to be excluded for any values of B quark mass.

Combination $B \rightarrow tW/bZ/bH^0$:

The ATLAS experiment has combined the various analyses targeted for specific decay modes to obtain the most sensitive limits on the pair production of B quarks [126]. The analyses using single lepton events, same sign charge dilepton events, events with opposite sign dilepton events, and multilepton events are combined to obtain lower limits on the mass of the B quark in the plane of $BR(B \rightarrow Wt)$ vs $BR(B \rightarrow bH)$. The searches were optimized for 100% branching fractions and hence are most sensitive at large $BR(B \rightarrow Wt)$, and also at large $BR(B \rightarrow bH^0)$. For all possible values of branching ratios in the three decay modes tW , bZ , or bH^0 , the lower limits on the B quark mass was found to be between 0.58 TeV and 0.81 TeV and as shown in Fig. 115.4. Analyses were also combined by the ATLAS experiment to provide the most sensitive limits on the pair production of B quarks to produce limits as a function of both B mass and branching ratio [125]. CMS provided similar combinations of their analyses.

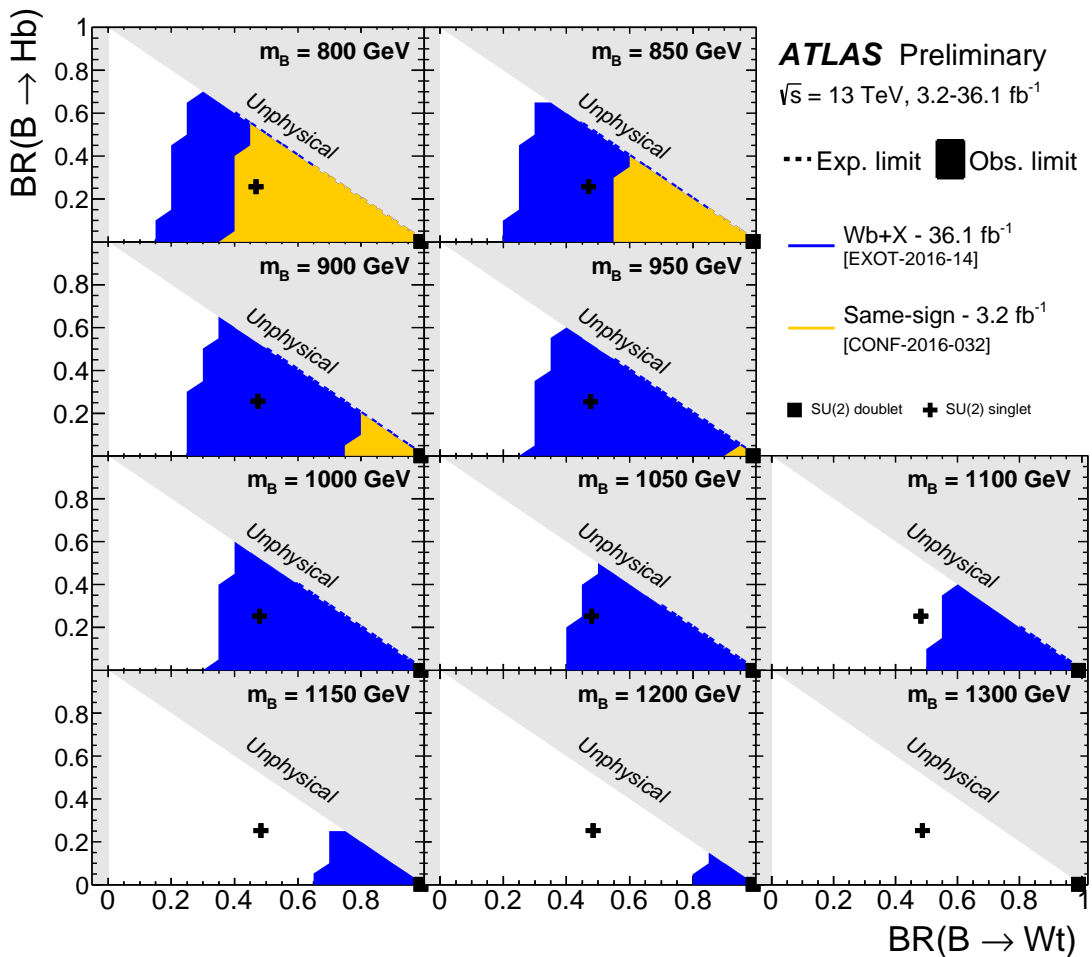


Figure 115.4: Observed limits on the mass of the B quark in the plane of $BR(B \rightarrow bH^0)$ versus $BR(B \rightarrow tW)$ from ATLAS searches for BB production [125]. Exclusion limits are drawn sequentially for each of the analyses and overlaid (rather than combined).

115.2.3.3. Searches for top-partner quark X :

Searches for a heavy top vector-like quark X , with exotic charge $5/3$, such as that proposed in Refs. 143,144, have been performed by both ATLAS and CMS [125,145].

The analyses assumed pair-production or single-production of X with X decaying with 100% branching fraction to tW . Searches for X have been performed using two final state signatures: same-sign leptons and lepton+jets.

The analysis based on searching for same-sign leptons, from the two W bosons from one of the X , has smaller backgrounds compared to the lepton+jets signature. Requiring same-sign leptons eliminates most of the standard model background processes, leaving those with smaller cross sections: $t\bar{t}$, W , $t\bar{t}Z$, WWW , and same-sign WW . In addition, backgrounds from instrumental effects due to charge misidentification were considered. Assuming pair production of X , the analyses by CMS using H_T as the discriminating variable restrict the X mass to be higher than 1.16 (1.10) TeV for a right (left) handed chirality particle [145,146,147]. The limits obtained by ATLAS, by classifying the signal region by number of b-jets, H_T , and missing p_T in the event, corresponded to a lower mass limit on X of 0.99 TeV [148,149].

Searches for X using leptons+jets final state signatures are based on either full or partial reconstruction of the T mass from the lepton, jets (including b jets) and missing p_T . The CMS search [145,150] also utilized jet substructure techniques to identify boosted X topologies. The discriminating variable used was the mass constructed from the lepton and b-tagged jet, $M_{(\ell,b)}$, which corresponds to the visible mass of leptonically decaying top quark. To optimize the search sensitivity, the events were further separated into categories based on lepton flavor (e, μ), the number of b-tagged jets, the number of W-tagged jets, and the number of t-tagged jets. In the absence of a signal, the CMS analysis excluded X quark masses with right-handed (left-handed) couplings below 1.32 (1.30) TeV [150].

The ATLAS lepton+jets search for X utilized events with high p_T W bosons and b-jets. The search described earlier for T pair production, with $T \rightarrow Wb$ decays, can be reinterpreted as a search for $X \rightarrow tW$. This analysis excluded X with masses below 1.25 TeV [125].

The single X production cross section depends on the coupling constant λ of the tWX vertex. ATLAS has performed an analysis of same-sign dileptons which includes both the single and pair production. This analysis led to a lower limit on the mass of the X of 0.75 TeV for both values of $\lambda = 0.5$ and 1.0 [151].

115.2.4. Colorons and Colored Scalars :

These particles are associated with top-condensate and top-seesaw models, which involve an enlarged color gauge group. The new particles decay to dijets, $t\bar{t}$, and $b\bar{b}$.

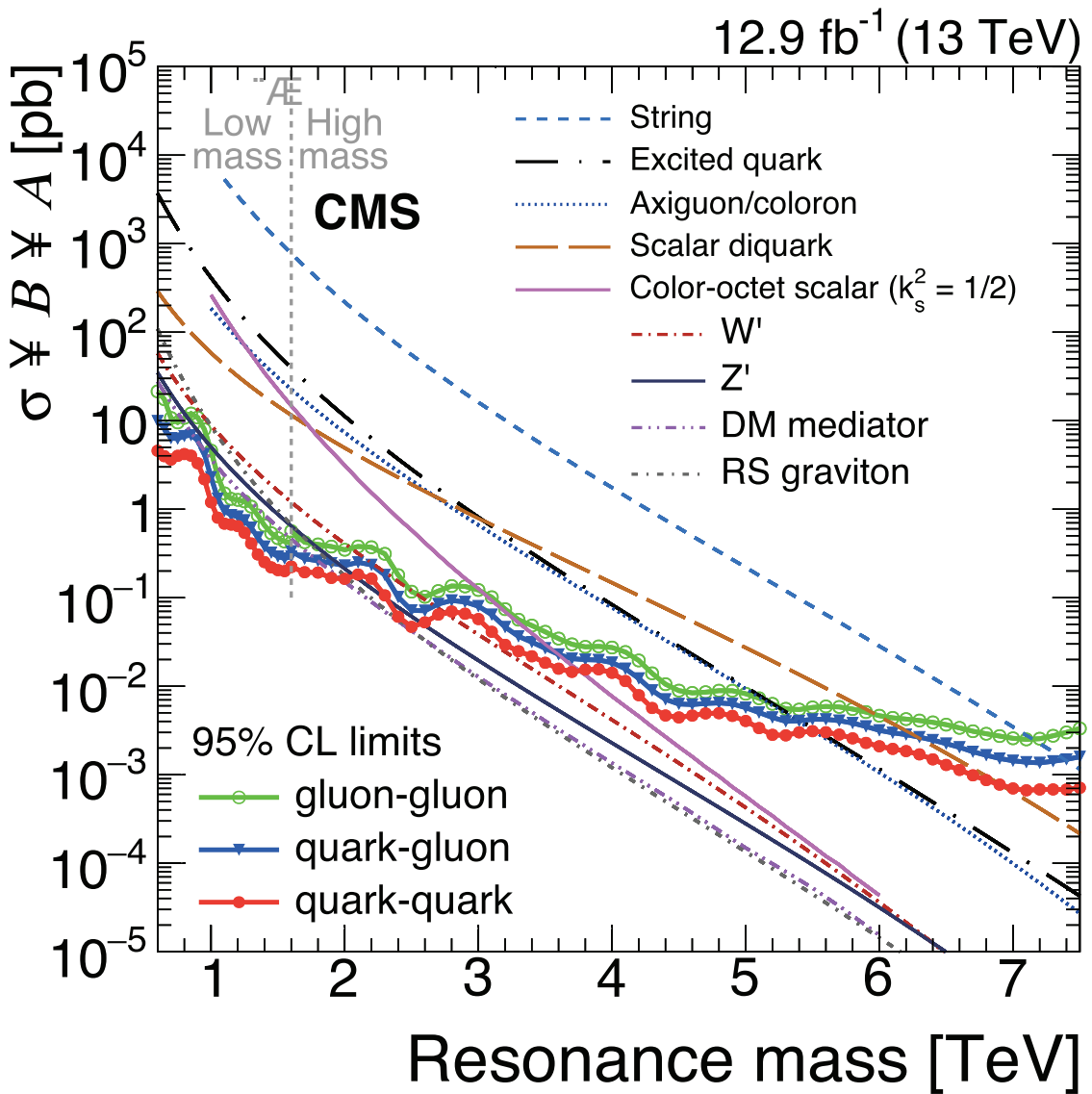


Figure 115.5: Observed 95% C.L. limits on $\sigma \times B \times A$ for string resonances, excited quarks, axigluons, colorons, E6 diquarks, s8 resonances, W' and Z' bosons, and Randall-Sundrum gravitons g_{KK} from [156].

Direct searches for colorons, color-octet scalars and other heavy objects decaying to $q\bar{q}$, qg , qq , or gg has been performed using LHC data from pp collisions at $\sqrt{s} = 7, 8$ and 13 TeV. Based on the analysis of dijet events from a data sample corresponding to a luminosity of 19.6 fb^{-1} , at $\sqrt{s} = 8 \text{ TeV}$ the CMS experiment excluded pair production of colorons with mass between $1.20 - 3.60$ and $3.90 - 4.08 \text{ TeV}$ [152]. Analyses of inclusive 8- and 10-jet final states with low missing transverse momentum by CMS [153], set limits in several benchmark models. Colorons (axigluons) with masses between 0.6 and 0.75 (up to 1.15) TeV were excluded, and gluinos in R-parity violating supersymmetric scenarios were ruled out from 0.6 up to 1.1 TeV.

A search for pair-produced colorons based on an integrated luminosity of 5.0 fb^{-1} at $\sqrt{s} = 7 \text{ TeV}$ by CMS excluded colorons with masses between 0.25 TeV and 0.74 TeV, assuming colorons decay 100% into $q\bar{q}$ [154]. This analysis was based on events with at least four jets and two dijet combinations with similar dijet mass. Color-octet scalars (s8) with masses between 1.20 – 2.79 TeV were excluded by CMS [152], and below 2.7 TeV by ATLAS [155].

These studies have now been extended to take advantage of the increased center-of-mass energy during Run 2 of the LHC. Using the 12.6 fb^{-1} of data collected at $\sqrt{s} = 13 \text{ TeV}$, searches for narrow resonances have been performed by CMS. An analysis of the dijet invariant mass spectrum formed using wide jets [156,157], separated by $\Delta\eta_{jj} \leq 1.3$, led to limits on new particles decaying to parton pairs (qq , qg , gg). Specific exclusions on the masses of colorons and color-octet scalars were obtained and are shown in Fig. 115.5.

115.3. Conclusions

As the above analyses have demonstrated, there is already substantial sensitivity to possible new particles predicted to accompany the H^0 in dynamical frameworks of electroweak symmetry breaking. No hints of any deviations from the standard model have been observed, and limits typically at the scale of a few hundred GeV to a few TeV are set.

Given the need to better understand the H^0 and to determine in detail how it behaves, such analyses continue to be a major theme of Run 2 the LHC, and we look forward to increased sensitivity as a result of the higher luminosity at the increased centre of mass energy of collisions.

References:

1. ATLAS Collab., Phys. Lett. **B716**, 1 (2012).
2. CMS Collab., Phys. Lett. **B716**, 30 (2012).
3. S. Weinberg, Physica A **96**, 327 (1979).
4. A. Manohar and H. Georgi, Nucl. Phys. **B234**, 189 (1984).
5. H. Georgi, Nucl. Phys. **B266**, 274 (1986).
6. R.S. Chivukula, hep-ph/0011264 (2000).
7. R.S. Chivukula, M.J. Dugan, and M. Golden, Phys. Rev. **D47**, 2930 (1993).
8. S. Weinberg, Phys. Rev. **D13**, 974 (1976).
9. S. Weinberg, Phys. Rev. **D19**, 1277 (1979).
10. L. Susskind, Phys. Rev. **D20**, 2619 (1979).
11. K. Lane, hep-ph/0202255 (2002).
12. C.T. Hill and E.H. Simmons, Phys. Reports **381**, 235 (2003), [Erratum-ibid. **390**, 553 (2004)].
13. R. Shrock, hep-ph/0703050 (2007).
14. E. Eichten *et al.*, Rev. Mod. Phys. **56**, 579 (1984) [Addendum-ibid. **58**, 1065 (1986)].
15. E. Eichten *et al.*, Phys. Rev. **D34**, 1547 (1986).
16. See “Status of Higgs Boson Physics” review in this volume..

17. R.S. Chivukula and V. Koulovassilopoulos, Phys. Lett. **B309**, 371 (1993).
18. R. Foadi, M.T. Frandsen, and F. Sannino, Phys. Rev. **D87**, 095001 (2013).
19. B. Holdom, Phys. Lett. **B150**, 301 (1985).
20. K. Yamawaki, M. Bando, and K.-i. Matumoto, Phys. Rev. Lett. **56**, 1335 (1986).
21. T.W. Appelquist, D. Karabali, and L.C.R. Wijewardhana, Phys. Rev. Lett. **57**, 957 (1986).
22. T. Appelquist and L.C.R. Wijewardhana, Phys. Rev. **D35**, 774 (1987).
23. T. Appelquist and L.C.R. Wijewardhana, Phys. Rev. **D36**, 568 (1987).
24. E. Gildener and S. Weinberg, Phys. Rev. **D13**, 3333 (1976).
25. Z. Chacko, R. Franceschini and R. K. Mishra, JHEP **1304**, 015 (2013).
26. B. Bellazzini *et al.*, Eur. Phys. J. **C73**, 2333 (2013).
27. B. Bellazzini *et al.*, Eur. Phys. J. **C74**, 2790 (2014).
28. Z. Chacko, R.K. Mishra, and D. Stolarski, JHEP **1309**, 121 (2013).
29. J.R. Ellis, M.K. Gaillard, and D.V. Nanopoulos, Nucl. Phys. **B106**, 292 (1976).
30. M.A. Shifman *et al.*, Sov. J. Nucl. Phys. **30**, 711 (1979) [Yad. Fiz. **30**, 1368 (1979)].
31. A.I. Vainshtein, V.I. Zakharov, and M.A. Shifman, Sov. Phys. Usp. **23**, 429 (1980) [Usp. Fiz. Nauk **131**, 537 (1980)].
32. M. Bando, K.-i. Matumoto, and K. Yamawaki, Phys. Lett. **B178**, 308 (1986).
33. W.D. Goldberger, B. Grinstein, and W. Skiba, Phys. Rev. Lett. **100**, 111802 (2008).
34. S. Matsuzaki and K. Yamawaki, Phys. Rev. **D85**, 095020 (2012).
35. S. Matsuzaki and K. Yamawaki, Phys. Rev. **D86**, 035025 (2012).
36. E. Eichten, K. Lane, and A. Martin, arXiv:1210.5462 (2012).
37. D.B. Kaplan and H. Georgi, Phys. Lett. **B136**, 183 (1984).
38. D.B. Kaplan, H. Georgi, and S. Dimopoulos, Phys. Lett. **B136**, 187 (1984).
39. M.E. Peskin, Nucl. Phys. **B175**, 197 (1980).
40. J. Preskill, Nucl. Phys. **B177**, 21 (1981).
41. R. Barbieri and A. Strumia, hep-ph/0007265 (2000).
42. N. Arkani-Hamed, A.G. Cohen, and H. Georgi, Phys. Lett. **B513**, 232 (2001).
43. N. Arkani-Hamed *et al.*, JHEP **0208**, 020 (2002).
44. N. Arkani-Hamed *et al.*, JHEP **0207**, 034 (2002).
45. M. Schmaltz and D. Tucker-Smith, Ann. Rev. Nucl. and Part. Sci. **55**, 229 (2005).
46. K. Agashe *et al.*, Phys. Lett. **B641**, 62 (2006).
47. P. Sikivie *et al.*, Nucl. Phys. **B173**, 189 (1980).
48. B. Bellazzini, C. Csaki, and J. Serra, Eur. Phys. J. **C74**, 2766 (2014).
49. R. Essig *et al.*, arxiv:1707.03399.
50. Z. Chacko, H. S. Goh and R. Harnik, Phys. Rev. Lett. **96**, 231802 (2006).
51. R.S. Chivukula, A.G. Cohen, and K.D. Lane, Nucl. Phys. **B343**, 554 (1990).
52. V.A. Miransky, M. Tanabashi, and K. Yamawaki, Phys. Lett. **B221**, 177 (1989) and Mod. Phys. Lett. **A4**, 1043 (1989).
53. W.A. Bardeen, C.T. Hill, and M. Lindner, Phys. Rev. **D41**, 1647 (1990).
54. C.T. Hill, Phys. Lett. **B266**, 419 (1991).
55. B.A. Dobrescu and C.T. Hill, Phys. Rev. Lett. **81**, 2634 (1998).
56. R.S. Chivukula *et al.*, Phys. Rev. **D59**, 075003 (1999).

57. S. Dimopoulos and L. Susskind, Nucl. Phys. **B155**, 237 (1979).
58. E. Eichten and K.D. Lane, Phys. Lett. **B90**, 125 (1980).
59. D.B. Kaplan, Nucl. Phys. **B365**, 259 (1991).
60. T. Appelquist, M. Piai, and R. Shrock, Phys. Rev. **D69**, 015002 (2004).
61. R.S. Chivukula, B.A. Dobrescu, and E.H. Simmons, Phys. Lett. **B401**, 74 (1997).
62. Y. Grossman and M. Neubert, Phys. Lett. **B474**, 361 (2000).
63. S.J. Huber and Q. Shafi, Phys. Lett. **B498**, 256 (2001).
64. T. Gherghetta and A. Pomarol, Nucl. Phys. **B586**, 141 (2000).
65. K. Agashe, R. Contino, and A. Pomarol, Nucl. Phys. **B719**, 165 (2005).
66. G.F. Giudice *et al.*, JHEP **0706**, 045 (2007).
67. R.S. Chivukula and H. Georgi, Phys. Lett. **B188**, 99 (1987).
68. G. D'Ambrosio *et al.*, Nucl. Phys. **B645**, 155 (2002).
69. K. Agashe *et al.*, hep-ph/0509117 (2005).
70. T. Appelquist and R. Shrock, Phys. Lett. **B548**, 204 (2002).
71. B. Keren-Zur *et al.*, Nucl. Phys. **B867**, 429 (2013).
72. J.M. Maldacena, Adv. Theor. Math. Phys. **2**, 231 (1998).
73. For a review, see C. Csaki, J. Hubisz, and P. Meade, hep-ph/0510275 (2005), and “Extra Dimensions” review in this volume.
74. C. Pica, PoS LATTICE **2016**, 015 (2016), arXiv:1701.07782.
75. T. Appelquist *et al.*, Phys. Rev. **D93**, 114514 (2016).
76. PDG review of Zprime boson in this volume.
77. PDG review of Wprime boson in this volume.
78. ATLAS Collab., arXiv:1707.02424 [hep-ex] , submitted to JHEP.
79. CMS Collab., CMS-PAS-EXO-16-031 (2016).
80. ATLAS Collab., Phys. Rev. **D90**, 052005 (2014).
81. ATLAS Collab., arXiv:1709.07242 [hep-ex] (2017).
82. CMS Collab., JHEP **0217**, 48 (2017).
83. CMS Collab., JHEP **0717**, 001 (2016).
84. ATLAS Collab., ATLAS-CONF-2016-014 (2016).
85. ATLAS Collab., arXiv:1703.09127 [hep-ex] , submitted to PRD.
86. CMS Collab., Phys. Lett. B 769,520(2017).
87. ATLAS Collab., Phys. Lett. B 759, 229 (2016).
88. CMS Collab., CMS-PAS-EXO-12-023 (2014).
89. ATLAS Collab., arXiv:1706.04786 [hep-ex] (2017).
90. ATLAS Collab., JHEP **1409**, 037 (2014).
91. CMS Collab., Phys. Lett. **B770**, 278 (2017).
92. CMS Collab., Phys. Lett. **B755**, 196 (2016).
93. CMS Collab., JHEP **1405**, 108 (2014).
94. CMS Collab., JHEP **1602**, 122 (2016).
95. CMS Collab., JHEP **1708**, 029 (2017).
96. CMS Collab., arXiv:arXiv:1708.08539 , submitted to Phys. Lett. B.
97. CMS Collab., CMS-PAS-JME-15-002, (2015), cds.cern.ch/record/2126325.
98. ATLAS Collab., Phys. Lett. **B743**, 235 (2015).
99. ATLAS Collab., Eur. Phys. J. **C75**, 165 (2015).

100. D. Pappadopulo, A. Thamm, R. Torre, and A. Wulzer, JHEP **1409**, 060 (2014).
101. ATLAS Collab., Phys. Lett. **B737**, 223 (2014).
102. CMS Collab., Phys. Lett. **B740**, 83 (2015).
103. ATLAS Collab., JHEP **1609**, 173 (2016).
104. ATLAS Collab., ATLAS-CONF-2017-051.
105. CMS Collab., arXiv:1705.09171 [hep-ex], submitted to Phys. Lett. B.
106. ATLAS Collab., arXiv:1708.04445 [hep-ex], submitted to Phys. Lett. B.
107. CMS Collab., arXiv:1708.05379 [hep-ex], submitted to Physical Review D.
108. ATLAS Collab., Phys. Lett. **B765**, 32 (2016).
109. ATLAS Collab., arXiv:1707.06958 [hep-ex], submitted to Phys. Lett. B.
110. CMS Collab., Phys. Lett. **B768**, 137 (2017).
111. CMS Collab., Eur. Phys. J. **C77**, 636 (2017).
112. ATLAS Collab., Eur. Phys. J. **C75**, 412 (2015).
113. ATLAS Collab., ATLAS-CONF-2016-049 (2016).
114. CMS Collab., CMS-EXO-12-053 (2015).
115. ATLAS Collab., ATLAS-CONF-2013-074 (2013).
116. ATLAS Collab., arXiv:1709.06783 [hep-ex], submitted to PLB (2017).
117. ATLAS Collab., <https://atlas.web.cern.ch/Atlas/GROUPS/PHYSICS/CombinedSummaryPlots/EXOTICS/index.html>.
118. CMS Collab., <https://twiki.cern.ch/twiki/bin/view/CMSPublic/PhysicsResultsB2GDibosons>.
119. F. del Aguila *et al.*, Nucl. Phys. **B334**, 1 (1990).
120. CMS Collab., CMS-PAS-B2G-17-003 (2017).
121. CMS Collab., CMS-PAS-B2G-12-017 (2014).
122. CMS Collab., Phys. Rev. **D93**, 012003 (2016) arXiv:1509.04177.
123. CMS Collab., CMS-PAS-B2G-12-013 (2015).
124. S.D. Ellis, C.K. Vermilion, and J.R. Walsh, Phys. Rev. **D80**, 051501 (2009).
125. ATLAS Collab., arXiv:1707.03347 [hep-ex].
126. ATLAS Collab., JHEP **1508**, 105 (2015).
127. CMS Collab., Phys. Lett. **B772**, 634 (2017).
128. ATLAS Collab., ATLAS-CONF-16-072 (2016), <http://cds.cern.ch/record/1480052>.
129. ATLAS Collab., Eur. Phys. J. **C76**, 442 (2016).
130. ATLAS Collab., ATLAS-CONF-2016-104 (2016), <http://cds.cern.ch/record/2220371>.
131. CMS Collab., Phys. Lett. **B729**, 149 (2014).
132. CMS Collab., JHEP **1506**, 080 (2015).
133. CMS Collab., arXiv:1706.03408 [hep-ex].
134. CMS Collab., cds.cern.ch/record/1709129 (2014).
135. CMS Collab., JHEP **1704**, 136 (2017).
136. CMS Collab., Phys. Lett. **B771**, 80 (2017).
137. ATLAS Collab., JHEP **1700**, 052 (2017) CERN-EP-2017-075, submitted to JHEP.
138. CMS Collab., arXiv:1708.01062 [hep-ex], Submitted to Phys. Lett. B.
139. ATLAS Collab., JHEP **1708**, 052, (2017).

140. CMS Collab., CMS-PAS-B2G-12-019 (2012),
<http://cds.cern.ch/record/1599436>.
141. CMS Collab., Phys. Rev. **D93**, 112009 (2016) arXiv:1507.07129.
142. ATLAS Collab., JHEP **1411**, 104 (2014).
143. R. Contino and G. Servant, JHEP **0806**, 026 (2008).
144. J. Mrazek, A. Wulzer, Phys. Rev. **D81**, 075006 (2010).
145. CMS Collab., JHEP **1708**, 073 (2017).
146. CMS Collab., CMS-PAS-B2G-16-019 (2017),
<https://cds.cern.ch/record/2256747>.
147. CMS Collab., Phys. Rev. Lett. **112**, 171801 (2014).
148. ATLAS Collab., ATLAS-CONF-16-03 (2016),
<http://cds.cern.ch/record/2161545>.
149. ATLAS Collab., Phys. Rev. **D91**, 112011 (2015).
150. CMS Collab., CMS-PAS-B2G-17-008 (2017),
<http://cds.cern.ch/record/2264686>.
151. ATLAS Collab., JHEP **1510**, 150 (2015).
152. V. Khachatryan *et al.* [CMS Collab.], Phys. Rev. **D91**, 052009 (2015).
153. CMS Collaboration, Phys. Lett. **B770**, 257 (2017).
154. CMS Collab., Phys. Rev. Lett. **110**, 141802 (2013).
155. ATLAS Collab., Phys. Rev. **D91**, 052007 (2015).
156. CMS Collaboration, Phys. Lett. **B769**, 520 (2017).
157. CMS Collab., CMS-PAS-EXO-15-001 (2015),
<https://cds.cern.ch/record/2048099>.